

Ulping/eng'gtcjgtv|'rwnguykj'2018'hgif'co rkwf gu'xc'eqjgtgpv' vcpulskqp'tcfkvlqp''

Dan Daranciang¹, John Goodfellow², Matthias Fuchs^{3,4}, Haidan Wen⁵, Shambhu Ghimire⁴,
David A. Reis^{3,4,6}, Henrik Loos⁷, Alan S. Fisher⁷, Aaron M. Lindenberg^{2,3,4*}

¹Department of Chemistry, Stanford University, Stanford, CA 94305

²Department of Materials Science and Engineering, Stanford University, Stanford, CA 94305

³Stanford Institute for Materials and Energy Science, SLAC National Accelerator Laboratory,
Menlo Park, CA 94025

⁴PULSE Institute for Ultrafast Energy Science, SLAC National Accelerator Laboratory, Menlo
Park, CA 94025

⁵Advanced Photon Source, Argonne National Laboratory, Argonne, IL 60439

⁶Department of Applied Physics, Stanford University, Stanford, CA 94305

⁷Linac Coherent Light Source, SLAC National Accelerator Laboratory, Menlo Park, CA 94025

We demonstrate terahertz pulses with field amplitudes exceeding 0.2 V/Å generated by coherent transition radiation. Femtosecond, relativistic electron bunches generated at the Linac Coherent Light Source are passed through a beryllium foil, and the emitted radiation is characterized as a function of the bunch duration and charge. Broadband pulses centered at a frequency of 10 THz with energies of 140 μJ are measured. These far-below-bandgap pulses drive a nonlinear optical response in a silicon photodiode, with which we perform nonlinear autocorrelations that yield information regarding the

terahertz temporal profile. Simulations of the spatiotemporal profile agree well with experimental results.

Ultrafast, high-intensity, single-cycle terahertz (THz) pulses have enabled techniques for coherent, atomic-scale control of materials and opened up opportunities for exploring nonlinear responses in materials¹⁻³. Recent progress in laser-based sources has led to pulse energies of roughly 10 μJ and field strengths of order 1 MV/cm for quasi-half-cycle pulses⁴⁻⁷, extending to greater than 10 MV/cm in the few-cycle regime⁸. Other approaches which use relativistic electron beams⁹⁻¹¹ have reached similar maximum pulse energies and field strengths¹²⁻¹⁶. Here, we present experimental results obtained by extracting coherent transition radiation (CTR) at the Linac Coherent Light Source (LCLS) free-electron laser¹⁷, using electron bunches as short as 50 fs. We observe THz pulses with energies exceeding 100 μJ , fields greater than 20 MV/cm at a focus, and bandwidth extending from 0.1 to 40 THz. Strong nonlinear responses are driven in a Si photodiode, which we use to carry out nonlinear autocorrelations of the THz radiation in a Michelson interferometer geometry. The measured spatial profile, spectrum, and pulse energy agree well with models of the CTR generation process.

Fig. 1(a) depicts a schematic of the experimental setup. Highly compressed, relativistic electron bunches with energies of 12 to 14.5 GeV were generated by the SLAC National Accelerator Laboratory linear accelerator at a repetition rate of 10 Hz or 60 Hz. These bunches had a total charge $q = 150$ to 350 pC and duration $\tau = 50$ to 200 fs full width at half maximum (FWHM), corresponding to peak currents of up to 7 kA. After being passed through the LCLS undulators, the bunches were propagated through a 2- μm -thick, 25-mm-diameter Be foil at a 45° angle of incidence, generating CTR in the forward (transmitted) and backward (downward) directions. The backward CTR exited the beamline vacuum into air through a 250- μm -thick, 25-

mm-diameter diamond window and was collimated by an off-axis parabolic gold-coated mirror with an effective focal length $f = 190$ mm. Field autocorrelations were performed in a Michelson interferometer, using a Si wafer as the beamsplitter and a pyroelectric detector. These measurements were intensity-normalized by the reflection from a different Si wafer and pyroelectric detector, located before the interferometer. A pyroelectric camera with 100- μm -sized pixels was used to measure the THz spot size. Pulse energies were measured with a thermopile power meter whose detector head was modified by bonding a 4-mm graphite disc over its metal absorbing surface. Complementary measurements of the extracted energy were obtained by measuring the energy loss of the electron beam due to emitted CTR. To perform nonlinear autocorrelations, we placed a Si photodiode (Thorlabs PDA100A) at the interferometer output. In all cases, the radiation propagated approximately 2 m in air before detection.

The intensity of CTR as a function of frequency, ω , is related to the form factor of the spatial charge distribution of the electron bunch, $f(\omega)$, via the following relationship¹⁸,

$$I(\omega) = N(N-1) I_e |f(\omega)|^2 \quad (\text{Eq. 1})$$

where $N = q/e$, I_e is the intensity of a single electron radiator, the $\sim N^2$ dependence reflects the constructive interference of the radiation emitted by each electron in the bunch, and $f(\omega)$ is the Fourier transform of the longitudinal charge distribution. For $q = 350$ pC and $\tau = 50$ fs, the measured pulse energy exceeded 140 μJ . We note that this measurement of τ likely represents an overestimate for the very shortest bunches due to the high-frequency cutoff of the spectrometer used to measure bunch duration at LCLS.

We systematically measured the pulse energy as a function of q and τ using a thermopile, time-average power meter. Because this detector measures temperature changes, it is sensitive over a broad spectral range, limited by absorption. As shown in Fig. 1(b), the pulse energy is

proportional to q^2/τ for $\tau > 50$ fs, consistent with the radiated field being proportional to the beam current, q/τ . The measured pulse energy for $\tau = 50$ fs exceeds what we would expect based on the longer pulses, consistent with an overestimate of the pulse duration due to the uncertainties described above.

In order to confirm the pulse energy measured by the power meter, the energy lost by the electron beam through CTR was determined¹⁷. This energy loss, measured to be 2.9 mJ for $q = 350$ pC and $\tau = 50$ fs [Fig. 1(c)], is not subject to uncertainties from power meter calibrations and sets an upper limit for the available energy. Several factors reduce the energy collected at the power meter to below the beam's energy loss: half of the CTR is forward-emitted; there is a ~30% reflection loss on the diamond window; and Coulomb scattering of the electron beam in the foil causes a loss we estimate as <0.1 mJ¹⁹. Additional losses are due to absorption of the THz in air along the 2-m propagation length²⁰, reflection and diffraction losses from the optics used, and surface reflections from the graphite layer deposited on the power meter.

We model the emitted THz electric fields in the slowly varying envelope approximation²¹ by propagating Laguerre-Gaussian modes through the optical setup²², including diffraction effects from the finite size of the foil and the other apertures in the beam path, but not taking absorption in air into account. Only modes with angular mode number equal to one were used, due to the radial polarization and symmetry of transition radiation. The initial electric field distribution at the Be foil is Fourier transformed into the frequency domain and decomposed into modes, and is given by the spatiotemporal distribution of the virtual photon field of a single electron at relativistic speed, convolved with the three-dimensional distribution of the electron beam. The spatiotemporal electron beam distribution was obtained by a start-to-end simulation of the entire LCLS accelerator using the Impact-T²³ and Elegant²⁴ codes. These simulations

predict the spatiotemporal THz distribution at the focus, shown in Figs. 2(a, i) and 2(b, i) for two bunch durations. Lineouts of these profiles in time [Figs. 2(a, ii) and 2(b, ii)] represent the temporal pulse shape at a given transverse position. They exhibit a central node due to the radial electric field polarization, and the peak field is found roughly 100 μm from the central axis. The predicted FWHM of 400 μm , for a reflective lens with $f = 150$ mm (roughly corresponding to a numerical aperture of 0.1), is in good agreement with the measured spatial profile using a pyroelectric camera [Fig. 1(d)], accounting for binning resulting from the 100 μm pixel size. We integrate over the simulated $q = 350$ pC, $\tau = 50$ fs profile, which predicts peak fields that reach 70 MV/cm [Fig. 2(a, ii)], to predict the maximum radiated energy:

$$U = \iiint c \epsilon_0 |E(r,t)|^2 r dr d\theta dt \quad (\text{Eq. 2})$$

A pulse energy of 560 μJ is obtained, within a factor of four of measured values. Scaling this to the measurement of 140 μJ per pulse yields peak fields at the focus of approximately 35 MV/cm.

Measured and calculated spectra for two bunch compressions are shown in Figs. 2(a, iii) and 2(b, iii). Notably, the $\tau = 50$ fs frequency spectrum is consistent with the generation of a quasi-half-cycle THz pulse. The experimentally measured interferograms from the Michelson interferometer [Figs. 2(a, iv) and 2(b, iv)] are limited by the pyroelectric LiTaO₃ detector used here, which has absorption edges in the 1-30 THz range^{25,26}. We retrieve the shown spectra by a Fourier transformation of the measured autocorrelation. Calculated spectra are obtained by a Fourier transform averaged over the transverse profile of the beam and further confirm the accuracy of our simulations.

The high intensities generated here enable the observation of a range of THz-induced nonlinear optical responses in solids^{1-3,27,28}. We observe fully saturated signals on Si photodiodes, even though the indirect bandgap of 1.1 eV (270 THz) is considerably higher than

the cutoff frequency of the source. Fig. 3(a) depicts a z -scan measurement, in which the photodiode current is monitored as a function of longitudinal position in the focused beam. Strongly nonlinear signals are observed within 10 mm of the focus, roughly matching the Rayleigh length at 10 THz. The 9.8 mm diameter of the diode was sufficient to fully collect the radiation in the shown range. Using a Ge crystal as a low-pass filter (bandgap 0.67 eV \approx 160 THz) did not affect the shape of the response, indicating that the near-infrared tails of the spectrum were not the dominant contributor.

Terahertz nonlinear autocorrelations^{29,30} were performed by placing a Si photodiode at the output of a Michelson interferometer. The result for a $q = 350$ pC, $\tau = 125$ fs electron bunch is shown in Fig. 3(b). To explain the shape, we simulate the (second-order) intensity autocorrelation of the THz emitted by an off-compression, double-horned electron bunch [Fig. 2(b, ii)], and the result is in Fig. 3(c). While direct knowledge of the nonlinear response is required to extract the most quantitative information, these photo-generated currents are likely a result of tunneling processes²⁸, impact ionization³, and ionization of defect states³¹. The match between Figs. 3(b) and 3(c) hints at a relatively simple method for measuring THz pulse shapes at high-field THz sources.

This work demonstrates a high-bandwidth THz source which reaches 140 μ J pulse energies and peak fields greater than 0.2 V/Å. Given the magnitude of the electron beam energy loss already observed, and upgrades which will increase the bunch charge, a clear path towards achieving fields in excess of 1 V/Å and pulse energies reaching 1 mJ is within reach. Finally, we note that the pulses generated here are extracted in a region at LCLS where the electron bunches are collinear with the FEL-generated x-rays, providing a clear path towards THz pump/x-ray probe measurements in the near future.

This work was carried out at the SLAC National Accelerator Laboratory (SLAC), which is operated for the U.S. Department of Energy (DOE) by Stanford University under Contract DE-AC02-76SF00515. The Linac Coherent Light Source is an Office of Science User Facility at SLAC. Experiments were supported by the U.S. DOE, Basic Energy Sciences, Materials Sciences and Engineering Division. J.G. was supported by a DOE Office of Science graduate fellowship program.

*e-mail: aaronl@stanford.edu

References

- ¹P. Gaal, W. Kuehn, K. Reimann, M. Woerner, T. Elsaesser, and R. Hey, *Nature* **450**, 1210–1213 (2007).
- ²T. Qi, Y. Shin, K. Yeh, K. Nelson, and A.M. Rappe, *Phys. Rev. Lett.* **102**, 247603 (2009).
- ³H. Wen, M. Wiczner, and A.M. Lindenberg, *Phys. Rev. B* **78**, 125203 (2008).
- ⁴F. Junginger, A. Sell, O. Schubert, B. Mayer, D. Brida, M. Marangoni, G. Cerullo, and R. Huber, *Opt. Lett.* **35**, 2645–2647 (2010).
- ⁵K. Kim, A. Taylor, J. Glowonia, and G. Rodriguez, *Nat. Photonics* **2**, 605–609 (2008).
- ⁶K.-L. Yeh, M.C. Hoffmann, J. Hebling, and K.A. Nelson, *Appl. Phys. Lett.* **90**, 171121 (2007).
- ⁷H. Hirori, A. Doi, F. Blanchard, and K. Tanaka, *Appl. Phys. Lett.* **98**, 091106 (2011).
- ⁸A. Sell, A. Leitenstorfer, and R. Huber, *Opt. Lett.* **33**, 2767–2769 (2008).
- ⁹M. Castellano, A. Cianchi, G. Orlandi, and V.A. Verzilov, *Nucl. Instrum. Methods Phys. Res., Sect. A* **435**, 297–307 (1999).
- ¹⁰G.L. Carr, M.C. Martin, W.R. McKinney, K. Jordan, G. Neil, and G. Williams, *Nature* **420**, 153–156 (2002).
- ¹¹T. Takahashi, Y. Shibata, F. Arai, K. Ishi, T. Ohsaka, M. Ikezawa, Y. Kondo, T. Nakazato, S. Urasawa, R. Kato, S. Niwano, and M. Oyamada, *Phys. Rev. E* **48**, 4674–4677 (1993).
- ¹²Y. Shen, T. Watanabe, D. Arena, C.C. Kao, J. Murphy, T. Tsang, X. Wang, and G. Carr, *Phys. Rev. Lett.* **99**, 043901 (2007).
- ¹³M. Gensch, L. Bittner, A. Chesnov, H. Delsim-Hashemi, M. Drescher, B. Faatz, J. Feldhaus, U. Fruehling, G. Geloni, C. Gerth, O. Grimm, U. Hahn, M. Hesse, S. Kapitzki, V. Kocharyan, O. Kozlov, E. Matyushevsky, N. Morozov, D. Petrov, E. Ploenjes, M. Roehling, J. Rossbach, E.

- Saldin, B. Schmidt, P. Schmueser, E. Schneidmiller, E. Syresin, A. Willner, and M. Yurkov, *Infrared Phys. Technol.* **51**, 423–425 (2008).
- ¹⁴J. van Tilborg, C. Schroeder, C. Tóth, C.G.R. Geddes, E. Esarey, and W.P. Leemans, *Opt. Lett.* **32**, 313–315 (2007).
- ¹⁵J. Park, C. Kim, J. Lee, C. Yim, C.H. Kim, J. Lee, S. Jung, J. Ryu, H.-S. Kang, and T. Joo, *Rev. Sci. Instrum.* **82**, 013305 (2011).
- ¹⁶S. Casalbuoni, B. Schmidt, P. Schmüser, V. Arsov, and S. Wesch, *Phys. Rev. ST Accel. Beams* **12**, 030705 (2009).
- ¹⁷P. Emma, R. Akre, J. Arthur, R. Bionta, C. Bostedt, J. Bozek, A. Brachmann, P. Bucksbaum, R. Coffee, F.-J. Decker, Y. Ding, D. Dowell, S. Edstrom, A. Fisher, J. Frisch, S. Gilevich, J. Hastings, G. Hays, P. Hering, Z. Huang, R. Iverson, H. Loos, M. Messerschmidt, A. Miahnahri, S. Moeller, H.-D. Nuhn, G. Pile, D. Ratner, J. Rzepiela, D. Schultz, T. Smith, P. Stefan, H. Tompkins, J. Turner, J. Welch, W. White, J. Wu, G. Yocky, and J. Galayda, *Nat. Photonics* **4**, 641–647 (2010).
- ¹⁸D. Mihalcea, C. Bohn, U. Happek, and P. Piot, *Phys. Rev. ST Accel. Beams* **9**, 082801 (2006).
- ¹⁹H.L. Anderson, editor, *A Physicist's Desk Reference* (Springer, 1989).
- ²⁰H. Cui, J. Yao, and C. Wan, *J. Phys.: Conf. Ser.* **276**, 012225 (2011).
- ²¹H. Kogelnik and T. Li, *Appl. Opt.* **5**, 1550–1567 (1966).
- ²²H. Loos, T. Borden, P. Emma, J. Frisch, and J. Wu, in *Proc. Part. Accel. Conf.* (Albuquerque, NM, 2007).
- ²³J. Qiang, S. Lidia, R. Ryne, and C. Limborg-Deprey, *Phys. Rev. ST Accel. Beams* **9**, 044204 (2006).
- ²⁴M. Borland, *Advanced Photon Source LS-287* (2000).

- ²⁵S. Kojima, H. Kitahara, S. Nishizawa, and M. Wada Takeda, *Jpn. J. Appl. Phys.* **42**, 6238–6241 (2003).
- ²⁶A.S. Barker, A.A. Ballman, and J.A. Ditzenberger, *Phys. Rev. B* **2**, 4233–4239 (1970).
- ²⁷J. Hebling, M.C. Hoffmann, H.Y. Hwang, K.-L. Yeh, and K.A. Nelson, *Phys. Rev. B* **81**, 035201 (2010).
- ²⁸W. Kuehn, P. Gaal, K. Reimann, M. Woerner, T. Elsaesser, and R. Hey, *Phys. Rev. B* **82**, 075204 (2010).
- ²⁹S. Winnerl, W. Seiwerth, E. Schomburg, J. Grenzer, K.F. Renk, C.J.G.M. Langerak, A.F.G. van der Meer, D.G. Pavel'ev, Y. Koschurinov, A.A. Ignatov, B. Melzer, V. Ustinov, S. Ivanov, and P.S. Kop'ev, *Appl. Phys. Lett.* **73**, 2983–2985 (1998).
- ³⁰G. Knippels, R. Mols, A. van der Meer, D. Oepts, and P. van Amersfoort, *Phys. Rev. Lett.* **75**, 1755–1758 (1995).
- ³¹S.D. Ganichev, I.N. Yassievich, W. Prettl, J. Diener, B.K. Meyer, and K.W. Benz, *Phys. Rev. Lett.* **75**, 1590–1593 (1995).

Figure captions

FIG. 1. (a) Schematic of the experimental setup. (b) The pulse energy collected by a thermopile power meter. (c) Electron beam energy loss due to insertion of the Be foil. (d) Lineouts of the focused THz spot. Inset: Pyrocam image.

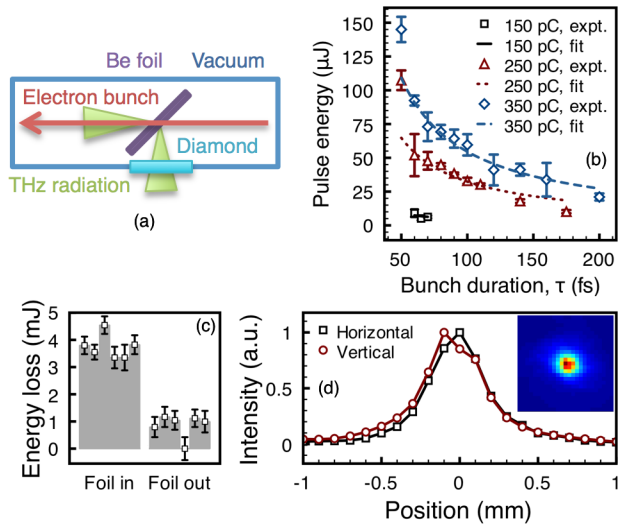


FIG. 2. Data for two bunch compressions. (a) $q = 350$ pC, $\tau = 50$ fs. (b) $q = 350$ pC, $\tau = 125$ fs. (i) Simulated spatiotemporal electric field profiles, (ii) simulated lineouts of the electric field near the focus, (iii) spectra, and (iv) measured Michelson autocorrelations.

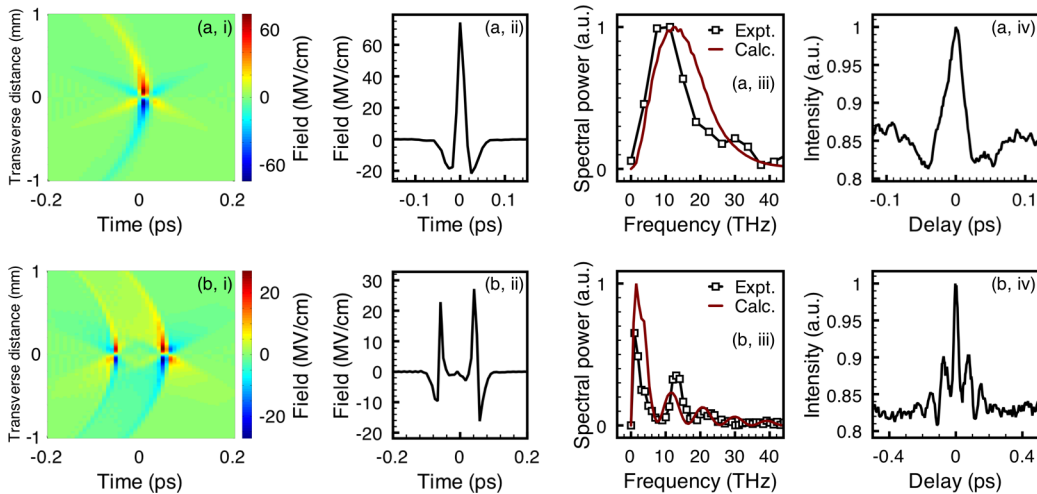


FIG. 3. (a) Scan along the propagation direction of a Si photodiode ($q = 350$ pC, $\tau = 81$ fs). (b) Nonlinear autocorrelation observed with a Si photodiode ($q = 350$ pC, $\tau = 125$ fs). (c) Simulated second-order autocorrelation for the electric field profile in Fig. 2(b, ii).

